

Research Article

Comparison of Methods for IKONOS Images Pan-sharpening Using Synthetic Sensors

Oscar Rosario Belfiore, Claudio Meneghini, Claudio Parente and Raffaele Santamaria
Department of Sciences and Technologies, University of Naples "Parthenope", Centro Direzionale,
Isola C4, Naples, 80143, Italy

Abstract: Many methods are present in literature for pan-sharpening of satellite images: they permit to transfer geometric resolution of panchromatic data to multispectral ones, but the results of their application are different. To evaluate the quality of these products, visual analysis is carried out, above all on the RGB composition to detect colour distortion. To quantize the level of similarity of the pan-sharpened images with them that should be achieved with effective more effective sensors, several indices are available such as: RMSE, correlation coefficients, UIQI, RASE. The principal limit of these indices consists in the terms of comparison because they compare the pan-sharpened images with the original ones that are with lower resolution. To supply the unavailability of the effective dataset with the same pixel dimensions of the pan-sharpened files, synthetic sensors can be introduced with lower resolution than the original ones. The correspondent degraded images can be submitted to pan-sharpening process and the results can be considered performed if similar to the original multispectral dataset. In this study IKONOS synthetic sensors are introduced to compare different methods: transforming the digital numbers into the radiance of the earth surface, original images of Campania Region are degraded and then submitted to some pan-sharpening approaches. The following methods are considered: multiplicative, simple mean, IHS, Fast IHS, Brovey, Weighted Brovey, Gram Schmidt, Zhang. Each resulting dataset is compared with the original multispectral one to evaluate the performance of each method.

Keywords: At sensor radiance, data fusion, performance evaluation, remote sensing

INTRODUCTION

As time passes, data fusion techniques become objects of important researches in the field of remote sensing image processing and they are widely implemented. The consequence is a continuous improvement of these methods in the last years. Sun-synchronous satellite sensors acquire concurrently images with different spectral and geometric resolutions: panchromatic (Pan) data have smaller pixel dimensions, but greater band width compared to the corresponding multispectral (MS) ones. Pan-sharpening is a data fusion approach that allows to get over this limit (Maglione *et al.*, 2014). The principal purpose is to improve multispectral data quality merging MS and Pan data, having both of them complementary spatial and spectral resolution (Chavez *et al.*, 1991; Wang *et al.*, 2005; Alparone *et al.*, 2007).

Several methods are available in literature and each of them produces specific images that are not the same originated by another. For this reason, the resulting pan-sharpened multispectral data must be evaluated: if visual analysis does not permit to detect colour distortions, quantitative evaluation is necessary.

Numerous comparisons between methods have been published (Thomas and Wald, 2005). To establish the best method so to prefer it in every case is very hard: the evaluation to be effective requires the availability of valid terms of comparison such as multispectral images with the same resolution of the pan-sharpened ones. This condition is difficult to achieve, so, according to Parente and Santamaria (2014) who proposed this approach for Landsat 7 ETM+ imagery, synthetic sensors (SynSs) must be considered.

In this study, IKONOS imagery (including pan as well as multispectral data) are considered. An example of the proposed approach for this type of data is also present in Santurri *et al.* (2010), but the authors in this case introduce the synthetic sensor degrading the matrices of Digital Numbers (DNs) instead of those concerning spectral radiance. In fact in this study we propose to define SynSs products by two steps: calculation of at-sensor spectral (or TOA, Top of Atmosphere) radiance and degradation of pixel sizes (atmospheric corrections are not considered because synthetic and real sensors are operative in the same conditions). The new images are involved in the pan-sharpening methods and the resulting TOA radiance matrices are converted in DN matrices: the obtained

Corresponding Author: Claudio Parente, Department of Sciences and Technologies, University of Naples "Parthenope", Centro Direzionale, Isola C4, Naples, 80143, Italy

This work is licensed under a Creative Commons Attribution 4.0 International License (URL: <http://creativecommons.org/licenses/by/4.0/>).

Table 1: Band range of Ikonos images

Bands	Resolution (m)	Range (μm)
Panchromatic	1	0.526-0.929
Blue	4	0.445-0.516
Green	4	0.506-0.595
Red	4	0.632-0.698
Near Infrared	4	0.757-0.853

scenes are matched with the corresponding original ones to verify their correctness.

DATA AND FIRST ELABORATIONS

Ikonos images: Launched into space on September 24 1999, Ikonos is a part of GeoEye's constellation satellites. It has a polar, circular, sun-synchronous 681-km orbit and both sensors have a swath width of 11 km. There are two types of sensors on board that acquire images in panchromatic band with 0.82 m resolution at nadir and in multispectral ones (Blue, Green, Red, Near Infrared) with 3.28 m resolution at nadir. Panchromatic

and multispectral images, all of these with a dynamic range of 11 bit, present cell sizes down-resampled respectively to 1 m and 4 m for commercial purposes (Digital Globe, 2013).

Ikonos imageries, because of their high level of spatial and spectral information, are useful for several studies: morphological configurations, urban environments (Herold *et al.*, 2002), land cover and use, forests, waters and other landscape elements (Gitas *et al.*, 2003). Map creation and updating (Belfiore and Parente, 2014) as well as the definition of the variation of shorelines in presence of coastal erosion (Basile Giannini *et al.*, 2011; Palazzo *et al.*, 2012) are examples of practical implementations of Ikonos imageries. (Table 1).

For this application an Ikonos scene, (panchromatic and multispectral data) acquired on 10/10/2005 at 09:59 GMT and concerning the Campania region, is used: it covers the municipalities of Bellona, Caiazzo, Capua, Caserta, Castel di Sasso, Castel Morrone, Piana di Monte Verna and Ponte Latone (Fig. 1).

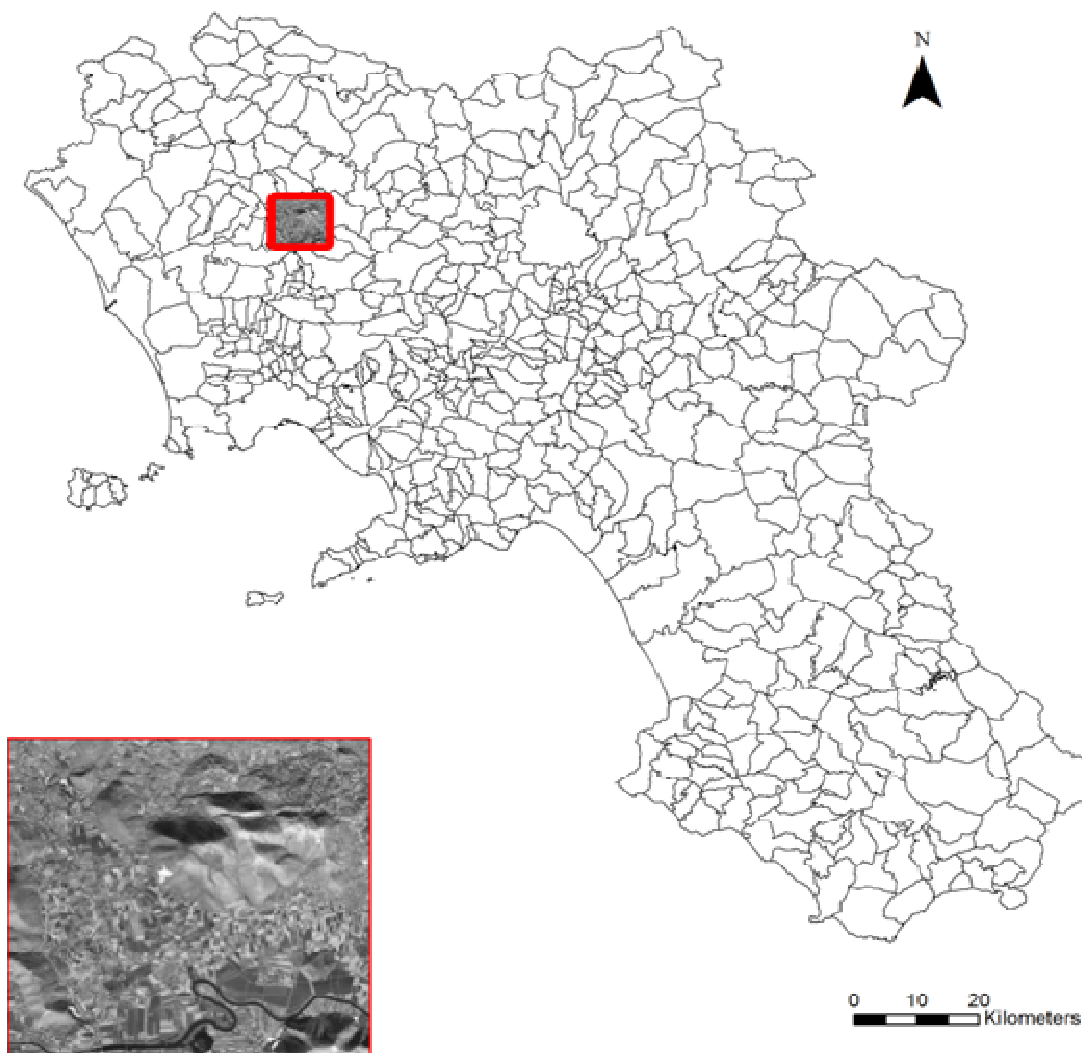


Fig. 1: The considered Ikonos scene and its location in Campania region

Table 2: Adopted values for the conversion from DN to radiance

Bands	CalCoef _λ	Bandwidth _λ
Panchromatic	161	403
Blu	728	71.3
Green	727	88.6
Red	949	65.8
Nir	843	95.4

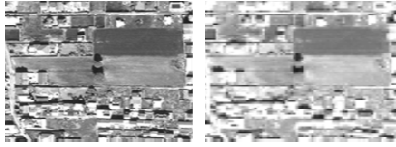


Fig. 2: Comparison between the original panchromatic band (left) and the degraded ones (right)

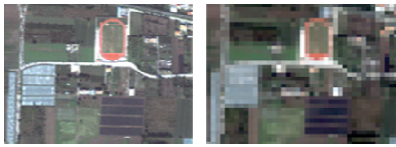


Fig. 3: Comparison between the RGB composition of the original multispectral bands (left) and the degraded ones (right)

Conversion of DNs to radiance: As previously mentioned, a transformation from DN to radiance values is required because they indicate how much of the power emitted by an emitting or reflecting surface will be received by an optical system looking at the surface from some angle of view (Borengasser *et al.*, 2008).

The following formula makes the transformation possible for the IKONOS images so to obtain at-sensor spectral radiance (TOA):

$$L_{\lambda} = \frac{10^4 \cdot DN_{\lambda}}{CalCoef_{\lambda} \cdot Bandwidth_{\lambda}} \quad (1)$$

where,

- L_{λ} = Radiance for spectral band λ at the sensor's aperture ($W/m^2/\mu m/sr$)
- DN_{λ} = The digital number of the pixel of the image
- $CalCoef_{\lambda}$ = The radiometric calibration coefficient [DN/(mW/cm^2-sr)]
- $Bandwidth_{\lambda}$ = Spectral band λ (nm)

The procedure is applied both to panchromatic and multispectral data: Taylor (2005) has determined the values of $CalCoef_{\lambda}$ and $Bandwidth_{\lambda}$ (Table 2) for Ikonos scenes acquired after 22/02/2001.

Reduction (downgrading) of geometric resolutions: The images, which are matrices of radiance, are down-sampled respectively from 4 m to 16 m (for multispectral bands) and from 1 m to 4 m (for panchromatic band). In this way it is possible to emulate images acquisition with SynS, having the same spectral bands of the original scenes but



Fig. 4: RGB composition of the multispectral degraded area

lower geometric resolutions. During the re-sampling, blocks of 16 pixels are replaced by one cell: its radiance value is derived by the average of the corresponding group. In Fig. 2 and 3 two details of the considered area are shown: the first relative to the pan images while the second concerning the multispectral data in RGB composition.

Calculation of new DNs values: The inverse of the stated previously formula permits to determine matrices of DNs from the re-sampled matrices of radiance:

$$DN = \frac{[L_{\lambda} \cdot (CalCoef_{\lambda} \cdot Bandwidth_{\lambda})]}{10^4} \quad (2)$$

Using a synthetic sensor, new scenes are obtained: they have identical position and the same acquisition time of IKONOS, but worse geometric resolutions.

PAN-SHARPENING METHODS

To apply pan-sharpening techniques, a clip of the synthetic sceneries selected. The considered area (Fig. 4) extends 8000 m × 8000 m (UTM/WGS84 plane coordinates -33T zone: $E_1 = 422640$ m; $N_1 = 4544772$ m; $E_2 = 430640$ m; $N_2 = 4536772$ m): It contains different elements like vegetation, building sand roads.

Eight pan-sharpening methods are applied to merge panchromatic and multispectral data: They are described in the following subsections.

Multiplicative: The pan-sharpened images are obtained by simple multiplications of each multispectral band for the panchromatic image using the following formula:

$$psh_i = \frac{Pan}{\mu_{Pan}} \cdot MS_i \quad (3)$$

where,

- psh_i = The pan-sharpened i th image
- Pan = The panchromatic image
- MS_i = The multispectral i th image
- μ_{Pan} = The mean of the pixel values of the panchromatic image

Klonus and Ehlers (2009) highlight the straightforwardness and simpleness of this algorithm. It contains spectral distortions (Crippen, 1987).

Simple mean: It is based on a simple mean between the panchromatic and each multispectral image (ESRI, 2012). The formula to compute the pan-sharpened image is:

$$psh_i = \frac{Pan+MS_i}{2} \quad (4)$$

IHS: Introduced by Carper *et al.* (1990), it is based on RGB to Intensity-Hue-Saturation (IHS) space transformation. The panchromatic image replaces the intensity component because of their similarity: therefore the inverse transformation is applied. R' G' B' components, having the same geometric resolution of panchromatic data, are determined using the succeeding equation:

$$\begin{bmatrix} R \\ G \\ B \end{bmatrix} = \begin{bmatrix} R + \delta \\ G + \delta \\ B + \delta \end{bmatrix} \quad (5)$$

where,

$$\delta = Pan - I \quad (6)$$

To calculate the I component all multispectral IKONOS bands are used:

$$I = \frac{\sum_{i=0}^n MS_i}{n} \quad (7)$$

Fast IHS: This method works in the same way of the IHS, but Intensity (I) is computed using weights. Tu *et al.* (2004) propose to use values of 0.75 and 0.25 for the green and the blue band, respectively: the weighting parameters are tested by the authors on 92 different IKONOS imageries. Similar numbers are obtained if the same approach proposed by Parente and Santamaria (2013) for Quickbird images and based on spectral response analysis is adopted for IKONOS ones; because NIR and Red are fully included in the panchromatic response, their weights are equal to the unit:

$$I = \frac{\sum_{i=0}^n w_i MS_i}{\sum_{i=0}^n w_i} \quad (8)$$

Brovoy: Described both by Pohl and van Genderen (1998), it is a pan-sharpening algorithm that preserves the relative spectral contributions of each pixel, but replaces its overall brightness with the high-resolution PAN image (Kalpoma and Kudoh, 2007). Each pan-sharpened image is obtained by n multispectral bands using the formula:

$$psh_i = \frac{Pan}{\sum_{i=0}^n MS_i} \cdot MS_i \quad (9)$$

Weighted brovov: As well as for FAST IHS, also for the Weighted Brovov method the same specific weights are introduced:

$$psh_i = \frac{Pan}{\sum_{i=0}^n w_i MS_i} \cdot MS_i \quad (10)$$

Zhang method: Introduced by Zhang (2004) and implemented in Geomatica 2015 by PCI Geomatics, this approach, statistics-based fusion, uses the least squares technique to correct grey values of the fused images according to those of the original Pan and MS images. It utilizes a set of statistic approaches to estimate the grey value relationship between all the input PAN and MS bands to automate the fusion process. Zhang (2002) affirms that his algorithm solves two major problems in image fusion: colour distortion and operator dependency.

Gram schmidt: Implemented by Laben and Brower (2000), the Gram Schmidt (GS) method is one of the most popular pan-sharpening technique: it maximizes image sharpness and minimize radiometric distortion better than other algorithms (Maurer, 2003). Averaging the multispectral bands it is possible to simulate a panchromatic band from the lower spatial resolution spectral bands. The second step consists in a Gram Schmidt transformation where both the simulated panchromatic data, employed as the first band and the multispectral bands are used. The first Gram Schmidt band is replaced by the high spatial resolution panchromatic band. In the last step, an inverse Gram Schmidt transformation is performed to create the pan-sharpened multispectral bands.

RESULTS

Eight fusion methods are tested on the considered down-sampled dataset: it covers different kinds of areas and its multispectral size is 500 by 500 pixels. In this study 32 pan-sharpened images are produced: their RGB composition, that includes necessary only 3 of the 4 multispectral images (NIR is not considered in the visualization), are shown in Fig. 5. Quantitative analysis is performed comparing the values of the following four quality indexes:

Root Mean Square Error (RMSE): Debated by Munehika *et al.* (1993), it calculates the difference of the standard deviation and the mean of the pan-sharpened and the original image. It estimates the spectral and spatial quality of the high resolution multispectral images (Rajendran and Vaithyanathan, 2012). A value closer to 0 indicates a good accuracy:

$$RMSE_{xy} = \sqrt{BIAS_{xy}^2 + \sigma_{xy}^2} \quad (11)$$

where, $BIAS_{xy}$ and σ_{xy} are respectively the difference between the mean and standard deviation values of the input multispectral image (x) and the output SynS image (y).

Correlation coefficient (ρ): Its value range varies from -1 to 1. A high correlation value means a good correspondence between the original bands and the corresponding fused ones. The formula is:

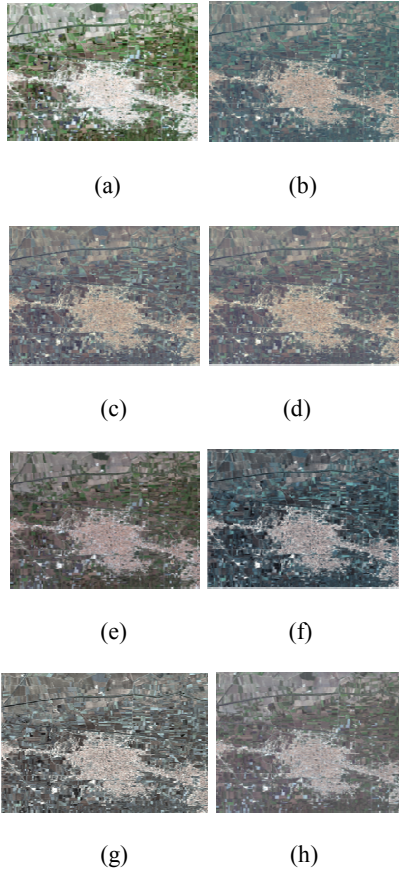


Fig. 5: RGB composition of the images derived by the following methods; (a): Brovey; (b): Weighted Brovey; (c): HIS; (d): FAST HIS; (e): Gram-Schmidt; (f): Multiplicative; (g): Simple Mean; (h): Zhang

$$\rho_{xy} = \frac{Cov_{xy}}{\sigma_x \sigma_y} \quad (12)$$

where,

- x = The input multispectral image
- y = The output pan sharpened image (SynS)
- Cov_{xy} = The covariance between x and y images
- σ_x and σ_y = The standard deviation of x and y images

Universal Image Quality Index (UIQI): Proposed by Wang and Bovik (2002), it evaluates the performance of the pan sharpened methods considering three factors such as loss of correlation, luminance and contrast distortion. It is obtained as:

$$UIQI_{xy} = \frac{Cov_{xy}}{\sigma_x \sigma_y} * \frac{2\mu_x 2\mu_y}{\mu_x^2 \mu_y^2} * \frac{2\sigma_x 2\sigma_y}{\sigma_x^2 \sigma_y^2} \quad (13)$$

where,

- μ_x = The mean value of image x
- μ_y = The mean value of image y

The ideal value of UIQI is 1

Table 3: Values of quality index for HIS

Bands	RMSE	$\rho_{xy}(CC)$	UIQI	RASE
Blue	43.148	0.715	0.696	
Green	40.907	0.866	0.864	
Red	44.579	0.893	0.885	
NIR	60.841	0.917	0.916	
	47.369	0.848	0.840	15.704

Table 4: Values of quality indexes for FAST HIS

Bands	RMSE	$\rho_{xy}(CC)$	UIQI	RASE
Blue	30.767	0.744	0.727	
Green	30.763	0.885	0.881	
Red	30.764	0.908	0.896	
NIR	30.769	0.921	0.916	
	30.766	0.864	0.855	10.061

Table 5: Values of quality indexes for Brovey

Bands	RMSE	$\rho_{xy}(CC)$	UIQI	RASE
Blue	41.882	0.733	0.717	
Green	42.082	0.866	0.864	
Red	39.734	0.919	0.904	
NIR	58.848	0.927	0.926	
	45.636	0.861	0.853	15.134

Table 6: Values of quality indexes for weighted Brovey

Bands	RMSE	$\rho_{xy}(CC)$	UIQI	RASE
Blue	40.321	0.763	0.751	
Green	40.775	0.884	0.881	
Red	39.404	0.927	0.908	
NIR	57.908	0.932	0.927	
	44.602	0.876	0.867	14.802

Table 7: Values of quality indexes for Simple Mean

Bands	RMSE	$\rho_{xy}(CC)$	UIQI	RASE
Blue	31.181	0.771	0.770	
Green	39.529	0.848	0.825	
Red	57.414	0.846	0.783	
NIR	93.345	0.892	0.096	
	55.367	0.839	0.618	19.720

Table 8: Values of quality indexes for multiplicative

Bands	RMSE	$\rho_{xy}(CC)$	UIQI	RASE
Blue	86.541	0.800	0.560	
Green	99.223	0.863	0.703	
Red	86.705	0.873	0.800	
NIR	118.026	0.883	0.821	
	97.623	0.855	0.721	32.201

Table 9: Values of quality indexes for Zhang

Bands	RMSE	$\rho_{xy}(CC)$	UIQI	RASE
Blue	22.940	0.857	0.840	
Green	33.950	0.884	0.862	
Red	42.760	0.885	0.865	
NIR	62.360	0.906	0.888	
	40.503	0.883	0.864	14.062

Table 10: Values of quality indexes for Gram-Schmidt

Bands	RMSE	$\rho_{xy}(CC)$	UIQI	RASE
Blue	16.167	0.742	0.718	
Green	28.686	0.697	0.672	
Red	32.756	0.724	0.698	
NIR	63.030	0.702	0.689	
	35.160	0.716	0.694	12.802

Relative Average Spectral Error (RASE): Discussed by Wald (2000) its value is expressed in percent and shows the average performance of a pan sharpened method considering all spectral bands:

$$RASE = \frac{100}{\mu} \sqrt{\frac{1}{n} \sum_{i=1}^n RMSE_i^2} \quad (14)$$

where,
 μ = The mean value of DN's of the n input images.

Considering indices values for all the fusion algorithms, which are reported in Table 3 to 9, it is possible to have an overview of the final results. (Table 10).

Even if the indices do not generate the same classification, it is evident that Fast IHS, GS, Zhang and Weighted Brovey produce the best performance. Multiplicative and Simple Mean methods are not reliable as confirmed by the results of low quality. The benefits of the introduction of weights are evident also for IHS and Brovey. Zhang is another valid pan-sharpening approach: adding a histogram matching among the fused images and the corresponding original ones, it improves, forcing a little, the final outcome.

CONCLUSION

The introduction of synthetic sensors to produce degraded images permits to apply to them different pan-sharpening methods determining if they are reliable or not. The conversion from DN's to at-sensor spectral radiance is needed: In this study it is supposed that the new sensors intercepts the same energy of the real sensor, but with different geometric resolutions. The equation to convert DN's into radiance for IKONOS images is present in literature and easy to apply.

The different pan-sharpening methods tested on an IKONOS multispectral scene acquired over Campania region in Italy present different results: not all of them have shown a good outcome. In literature problems and limitations of each pan-sharpening method are described by several studies (Wald *et al.*, 1997; Du *et al.*, 2007). This study suggests an approach to support performance evaluation. It is proved that, giving weights to each multispectral band to differentiate their rule in pan-sharpening process, possibility to achieve good results increases a lot.

Considering that this approach classifies performances of each method, it can be used to test new data fusion algorithms and procedures. In this study pixel dimensions are quadrupled, but also other transformations of cell sizes can be considered; in this manner is possible to determine the performance of each method in reference to increasing levels of spatial resolution.

ACKNOWLEDGMENT

This research is included in the Project "Innovative and emerging geomatics techniques of survey, remote sensing (by airplane, satellite, UAV) and WEBGIS for risk mapping in real time and the prevention of

environmental damage" supported by the research funding of Research Projects of National Interest (PRIN) 2010-2011⁴. The fund is managed by MIUR (Ministero dell'Istruzione, dell'Università e della Ricerca), the Italian Ministry of Instruction, University and Research.

REFERENCES

- Alparone L., L. Wald, J. Chanussot, C. Thomas, P. Gamba and L.M. Bruce, 2007. Comparison of pansharpening algorithms: Outcome of the 2006 GRS-S data-fusion contest. *IEEE T. Geosci. Remote*, 45(10): 3012-3021.
- Basile Giannini, M., C. Parente, P. Maglione and R. Santamaria, 2011. Cartography and remote sensing for coastal erosion analysis. *Proceedings of Coastal Process II*. In: Benassai, G., C.A. Brebbia and G. Rodriguez (Eds.), Naples (Italy), WIT Transactions on Ecology and the Environment. WIT Press, ISBN: 978-1-84564-534-2, pp: 65-76.
- Belfiore, O.R. and C. Parente, 2014. Comparison of different methods to rectify IKONOS imagery without use of sensor viewing geometry. *Am. J. Remote Sens.*, 2(3): 15-19.
- Borengasser, M., W.S. Hungate and R. Watkins, 2008. *Hyperspectral Remote Sensing-Principles and Applications*. CRC Press, Boca Raton, FL.
- Carper, W.J., T.M. Lillesand and R.W. Kiefer, 1990. The use of intensity-hue-saturation transformations for merging SPOT panchromatic and multispectral image data. *Photogramm. Eng. Rem. S.*, 56: 459-467.
- Chavez, P., S.C. Sides and J.A. Anderson, 1991. Comparison of three different methods to merge multiresolution and multispectral data Landsat TM and SPOT panchromatic. *Photogramm. Eng. Rem. S.*, 57(3): 295-303.
- Crippen, R.E., 1987. A simple spatial filtering routine for the cosmetic removal of scan-line noise from LANDSAT TM P-tape imagery. *Photogramm. Eng. Rem. S.*, 55(3): 327-331.
- Digital Globe, 2013. IKONOS Data Sheet. Retrieved from: www.digitalglobe.com/sites/default/files/DG_IKONOS_DS.pdf. (Accessed on: May 29, 2015)
- Du, Q., N.H. Younan, R. King and V.P. Shah, 2007. On the performance evaluation of pan-sharpening techniques. *IEEE Geosci. Remote S.*, 4: 518-522.
- ESRI, 2012. *Fundamentals of Panchromatic Sharpening*. Retrieved from: <http://resources.arcgis.com/en/help/main/10.1/index.html#//009t000000mw000000>. (Accessed on: May 29, 2015)
- Gitas, I.Z., C.G. Karydas and G.V. Kazakis, 2003. Land covermapping of mediterranean landscapes, sing SPOT4 Xi and IKONOS imagery-preliminary investigation. *Options Mediterran.*, 46: 27-41.

- Herold, M., J. Scepan, A. Müller and S. Günther, 2002. Objectoriented mapping and analysis of urban and use/cover using IKONOS data. Proceeding of 22nd EARSEL Symposium, Geoinformation for European-wide Integration. Prague, June 04-06, pp: 531-538.
- Kalpoma, K.A. and J.I. Kudoh, 2007. Image fusion processing for IKONOS 1-m color imagery. *IEEE T. Geosci. Remote*, 45(10): 3075-3086.
- Klonus, S. and M. Ehlers, 2009. Performance of evaluation methods in image fusion. Proceeding of the IEEE 12th International Conference on Information Fusion. Seattle, USA, pp: 1409-1416.
- Laben, C.A. and B.V. Brower, 2000. Process for enhancing the spatial resolution of multispectral imagery using pan-sharpening. Technical Report US Paten No. 6,011,875.
- Maglione, P., C. Parente and A. Vallario, 2014. Coastline extraction using high resolution WorldView-2 satellite imagery. *Eur. J. Remote Sens.*, 47: 685-699.
- Maurer, T., 2013. How to pan-sharpen images using the Gram-Schmidt pan-sharpen method-a recipe. Proceeding of the International Archives of the Photogrammetry, Remote Sensing and Spatial Information Sciences. Hannover, Germany, pp: 239-244.
- Munehika, C.K., J.S. Warnick, C. Salvaggio and J.R. Schott, 1993. Resolution enhancement of multispectral image data to improve classification accuracy. *Photogramm. Eng. Rem. S.*, 59(1): 67-72.
- Palazzo, F., D. Latini, V. Baiocchi, F. Del Frate, F. Giannone, D. Dominici and S. Remondiere, 2012. An application of COSMO-Sky Med to coastal erosion studies. *Eur. J. Remote Sens.*, 45: 361-370.
- Parente, C. and R. Santamaria, 2013. Increasing geometric resolution of data supplied by quickbird multispectral sensors. *Sens. Trans.*, 156(9): 111-115.
- Parente, C. and R. Santamaria, 2014. Synthetic sensor of landsat 7 ETM+ imagery to compare and evaluate pan-sharpening methods. *Sens. Trans.*, 177(8): 294-301.
- Pohl, C. and J. van Genderen, 1998. Multisensor image fusion in remote sensing: Concepts, methods and applications. *Int. J. Remote Sens.*, 19(5): 823-854.
- Rajendran, V. and V. Vaithiyanathan, 2012. Improved pansharpening method. *Res. J. Appl. Sci. Eng. Technol.*, 4(24): 5464-5468.
- Santurri, L., R. Carlà, F. Fiorucci, B. Aiazzi, S. Baronti, M. Cardinali and A. Mondini, 2010. Assessment of very high resolution satellite data fusion techniques for landslide recognition. In: Wanger, W. and B. Szekely (Eds.), *ISPRS TC VII Symposium*. Vienna, Austria, pp: 492-496.
- Taylor, M., 2005. *IKONOS Planetary Reflectance and Mean Solar Exoatmospheric Irradiance*; Space Imaging Inc., Thornton, Colorado (USA).
- Thomas, C. and L. Wald, 2005. Assessment of the quality of fused products. In: Dubrovnik Croatia, O. (Eds.), *Proceeding of the 24th EARSeL Symposium "New Strategies for European Remote Sensing"*. Balkema, May 25-27, pp. 317-325.
- Tu, T.M., P.S. Huang, C.L. Hung and C.P. Chang, 2004. A fast intensity-hue-saturation fusion technique with spectral adjustment for IKONOS imagery. *IEEE Geosci. Remote S.*, 1(4): 309-312.
- Wald, L., 2000. Quality of high resolution synthesized images: Is there a simple criterion? Proceeding of the International Conference Fusion of Earth Data. Nice (France). January 26-28, pp: 99-105.
- Wald, L., T. Ranchin and M. Mangolini, 1997. Fusion of satellite images of different spatial resolutions: Assessing the quality of resulting images. *Photogramm. Eng. Rem. S.*, 63(6): 691-699.
- Wang, Z. and A.C. Bovik, 2002. A universal image quality index. *IEEE T. Geosci. Remote*, 9(3): 81-84.
- Wang, Z., D. Ziou, C. Armenakis, D. Li and Q. Li, 2005. A comparative analysis of image fusion methods. *IEEE T. Geosci. Remote*, 43(6): 1391-1402.
- Zhang, Y., 2002. A new automatic approach for effectively fusing Landsat 7 as well as IKONOS images. Proceeding of the IEEE/IGARSS'02. Toronto (Canada), June 24-28.
- Zhang, Y., 2004. Understanding image fusion. *Photogramm. Eng. Rem. S.*, 70(6): 657-661.